

Solution space heterogeneity of the random K -satisfiability problem: Theory and simulations

Haijun Zhou^{1,2}

¹Key Laboratory of Frontiers in Theoretical Physics, Institute of Theoretical Physics, Chinese Academy of Sciences, Beijing 100190, China

²Kavli Institute for Theoretical Physics China (KITPC) at the Chinese Academy of Sciences, Beijing 100190, China

E-mail: zhouhj@itp.ac.cn

Abstract. The random K -satisfiability (K -SAT) problem is an important problem for studying typical-case complexity of NP-complete combinatorial satisfaction; it is also a representative model of finite-connectivity spin-glasses. In this paper we review our recent efforts on the solution space fine structures of the random K -SAT problem. A heterogeneity transition is predicted to occur in the solution space as the constraint density α reaches a critical value α_{cm} . This transition marks the emergency of exponentially many solution communities in the solution space. After the heterogeneity transition the solution space is still ergodic until α reaches a larger threshold value α_d , at which the solution communities disconnect from each other to become different solution clusters (ergodicity-breaking). The existence of solution communities in the solution space is confirmed by numerical simulations of solution space random walking, and the effect of solution space heterogeneity on a stochastic local search algorithm SEQSAT, which performs a random walk of single-spin flips, is investigated. The relevance of this work to glassy dynamics studies is briefly mentioned.

1. Introduction

A random K -Satisfiability (K -SAT) formula is constructed by adding M constraints on N variables [1]. Each variable i has a spin state $\sigma_i = \pm 1$, and each constraint a applies to K different variables that are randomly chosen from the whole set of variables. The energy of constraint a is expressed as

$$E_a = \prod_{i \in \partial a} \left[\frac{1 - J_a^i \sigma_i}{2} \right], \quad (1)$$

where ∂a denotes the set of variables involved in constraint a (the size of ∂a is K), $J_a^i = \pm 1$ is the preferred spin state of constraint a on variable i . Each of the K preferred spin values J_a^i of a constraint a are randomly and independently assigned a value $+1$ or -1 with equal probability. The whole set $\{J_a^i\}$ of preferred spin values are then fixed, but the actual spin state σ_i of each variable i is allowed to change. The constraint energy E_a is zero if at least one of the variables $i \in \partial a$ takes the spin value $\sigma_i = J_a^i$, otherwise $E_a = 1$. Given a random K -SAT formula, the task is to construct at least one spin configuration $\vec{\sigma} \equiv \{\sigma_1, \sigma_2, \dots, \sigma_N\}$ that satisfies all the constraint (i.e., makes all the constraint energy E_a to be zero), or to prove that no such solutions (i.e., satisfying spin configurations) exist.

When N is large, rigorous mathematical proofs (see, e.g., review article [2]) and numerical simulations [1] revealed that whether a random K -SAT formula is satisfiable or not depends on the constraint density α ($\equiv M/N$). As α increases beyond certain satisfiability threshold $\alpha_s(K)$, the probability of a randomly constructed K -SAT formula to be satisfiable quickly drops from being close to unity to being close to zero. Among the whole ensemble of random K -SAT formulas, the satisfiability of those instances with constraint density α in the vicinity of $\alpha_s(K)$ is the hardest to determine. This empirical observation has stimulated a lot of investigations.

The random K -SAT problem was intensively studied in the statistical physics community during the last decade [3, 4, 5, 6, 7]. The number of solutions for the random K -SAT problem as a function of constraint density was calculated in Ref. [3] by the replica method of spin-glass physics. Later the satisfiability threshold α_s as a function of K was calculated by the first-step replica-symmetry-breaking (1RSB) energetic cavity method [4, 8]. The evolution of the solution space of the random K -SAT problem with constraint density α was studied in Refs. [5, 9, 10] using the 1RSB entropic cavity method [11, 12]. Before the satisfiability threshold $\alpha_s(K)$ is reached, the solution space experiences a clustering transition at $\alpha = \alpha_d(K)$, where exponentially many solution clusters (Gibbs states) form and the ergodicity of the solution space is broken. This clustering transition is followed by a condensation transition at $\alpha = \alpha_c(K) \geq \alpha_d(K)$, where a sub-exponential number of solution clusters begin to dominate the solution space. Within a solution cluster, the spin states of a large fraction of variables start to be frozen to the same value as α exceeds certain threshold value α_f that may be different for different clusters. The freezing transition was investigated in Refs. [9, 13, 14]. Some of these phase transitions (i.e., the clustering and the condensation transition) were earlier found to occur in mean-field p -body-interaction spin glasses [15], with temperature T (instead of the constraint density) being the control parameter.

In the present paper, we review our recent efforts on the solution space fine structures of the random K -SAT problem. A heterogeneity transition is predicted to occur in the solution space as the constraint density α reaches a critical value $\alpha_{cm}(K)$ which is smaller than $\alpha_d(K)$ [16]. This transition marks the emergency of exponentially many solution communities in the solution space. For $\alpha_{cm} < \alpha < \alpha_d$, the heterogeneous solution space is ergodic; at $\alpha = \alpha_d$ the solution communities will turn into different solution clusters as an ergodicity-breaking transition occurs. The existence of solution communities in the solution space is confirmed by numerical simulations on single K -SAT formulas [17], and the effect of solution space heterogeneity on a stochastic local search algorithm SEQSAT, which performs a random walk of single-spin flips, is investigated [18]. Beyond the clustering transition point α_d , our numerical simulation results [17, 19] suggested that the individual solution clusters of the solution space also have rich internal structures.

The replica-symmetric cavity method is used in the next section to calculate the value of α_{cm} for the onset of solution space structural heterogeneity. Section 3 presents the data-clustering results on sampled solutions of single random K -SAT formulas; Section 4 reports the simulation results of the stochastic search algorithm SEQSAT. We conclude this work in Sec. 5 and point out some possible links with the phenomena of two-step relaxation and dynamical heterogeneity in supercooled liquids.

2. Solution space heterogeneity transition

Given a random K -SAT formula, the total energy $E(\vec{\sigma}) \equiv \sum_a E_a$ is equal to the number of violated constraints by the spin configuration $\vec{\sigma}$. The whole set \mathcal{S} of spin configurations with $E(\vec{\sigma}) = 0$ form the solution space of this K -SAT formula. The similarity between any two

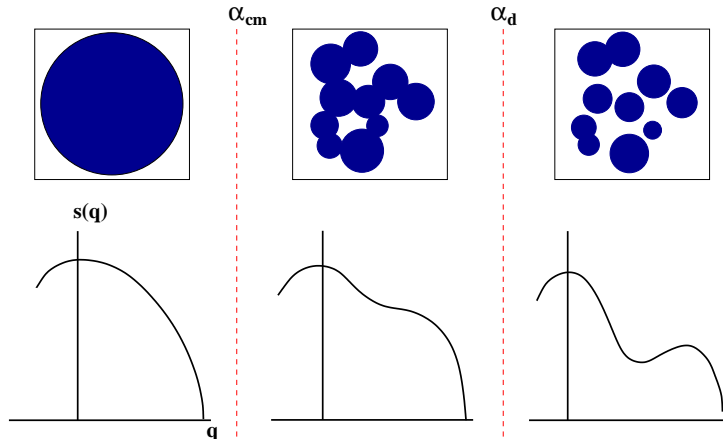


Figure 1. Detecting heterogeneity of the solution space by the shape of the entropy density function $s(q)$: At low constraint density α (left panel), $s(q)$ is a concave function of the solution-pair overlap q . Solution communities start to form as α exceeds a threshold value α_{cm} (middle panel) and the solution space becomes heterogeneous; this makes $s(q)$ to be non-concave. At the clustering transition point α_d (right panel), solution communities separate into different clusters, and $s(q)$ becomes non-monotonic. As α further increases, solution-pairs with intermediate overlap values may cease to exist and then $s(q) = -\infty$ for these intermediate q values.

solutions $\vec{\sigma}^1$ and $\vec{\sigma}^2$ of the space \mathcal{S} can be measured by an overlap parameter defined as

$$q(\vec{\sigma}^1, \vec{\sigma}^2) = \frac{1}{N} \sum_{i=1}^N \sigma_i^1 \sigma_i^2. \quad (2)$$

To characterize the statistical property of the solution space, we count the total number of solution-pairs with overlap value q and denote this number as $\mathcal{N}(q)$. For a random K -SAT formula of size $N \geq 1$ and constraint density $\alpha < \alpha_s(K)$, the size of \mathcal{S} is exponential in N , and $\mathcal{N}(q)$ is also exponential in N . It is helpful to define an entropy density $s(q)$ as $s(q) \equiv (1/N) \ln[\mathcal{N}(q)]$.

The solution space \mathcal{S} has a natural graphical representation (solution graph), in which each solution is denoted as a node and two nodes are connected by an edge if (and only if) the corresponding solutions are interchangeable by a single-spin flip. When α is less than the clustering transition point $\alpha_d(K)$, this solution graph has only a single connected component (solution cluster) that contains all (or almost all) of the solutions [5]. As is well known in social and biological network studies (see, e.g., Refs. [20, 21]), a connected network component may have rich internal community structures. A community of a graph refers to a subset of nodes of the graph that are much more densely inter-connected with each other than with the remaining nodes of the graph. If communities exist in the solution graph of a large random K -SAT formula, many subsets of solutions (solution communities) can then be extracted, with the property that each solution community contains a set of solutions that are much more similar with each other than with the other solutions. If such solution communities are abundant and of considerable sizes, they will be statistically relevant and will be manifested in the form of the entropy density function $s(q)$ (see Fig. 1).

We define a partition function $Z(x)$ as

$$Z(x) \equiv \sum_{\vec{\sigma}^1 \in \mathcal{S}} \sum_{\vec{\sigma}^2 \in \mathcal{S}} \exp(Nxq(\vec{\sigma}^1, \vec{\sigma}^2)) = \sum_q \exp[N(s(q) + xq)], \quad (3)$$

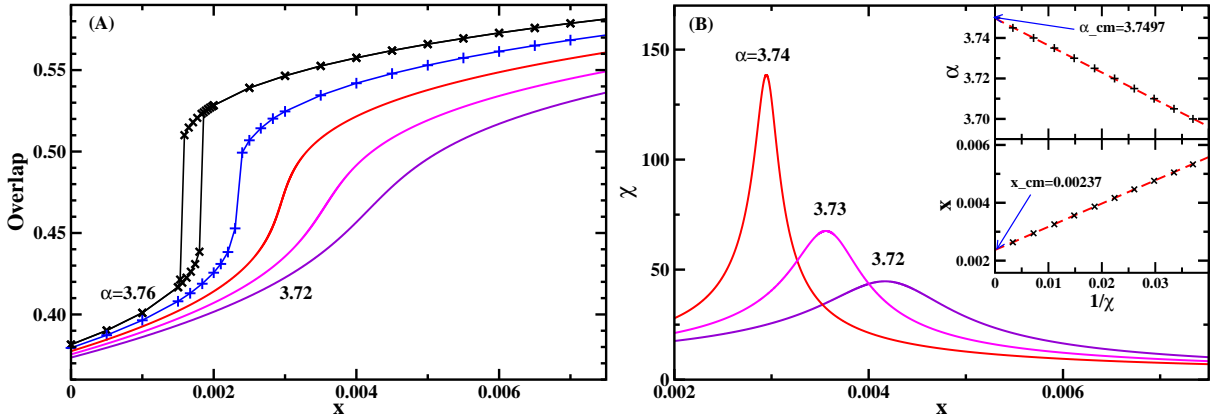


Figure 2. The mean overlap $\bar{q}(x)$ and the susceptibility $\chi(x)$ at constraint density value α for the random 3-SAT problem. In (A) α increases from 3.72 to 3.76 (right to left) with step size 0.01. The insets of (B) demonstrate that the peak value of χ diverges inverse linearly with α and x as the critical point ($\alpha_{cm} = 3.7497$, $x_{cm} = 0.0024$) is approached.

where x is an auxiliary binding field. The free entropy $\Phi(x)$ of the system is defined as $\Phi(x) \equiv \ln Z(x)$. In the thermodynamic limit of $N \rightarrow \infty$, the free entropy density $\phi(x) \equiv \Phi(x)/N$ is related to the entropy density $s(q)$ by

$$\phi(x) = \max_{q \in [-1, 1]} [s(q) + xq] = s(\bar{q}(x)) + x\bar{q}(x). \quad (4)$$

In Eq. (4), $\bar{q}(x)$ is the mean value of solution-solution overlaps under the binding field x , it is the argument value at which the function $s(q) + xq$ reaches the global maximum.

If the entropy density $s(q)$ is a concave function of $q \in [q_0, 1]$ (Fig. 1, left panel), where q_0 is the most probable solution-pair overlap value, then for each $x \geq 0$ there is only one mean overlap \bar{q} , and $\bar{q}(x)$ is a continuous function of x . On the other hand, if $s(q)$ is non-concave in $q \in [q_0, 1]$ (Fig. 1, middle and right panel), then the value of $\bar{q}(x)$ changes discontinuously at certain value of $x = x^* > 0$. We have exploited this correspondence between the non-concavity of $s(q)$ and the discontinuity of $\bar{q}(x)$ to determine the threshold constraint density α_{cm} at which $s(q)$ starts to be non-concave [16]. We regard $\alpha = \alpha_{cm}$ as the point at which the solution space of the random K -SAT problem transits into structural heterogeneity. This is because, as schematically shown in Fig. 1, at α_{cm} it starts to make sense to distinguish between intra-community overlap values and inter-community overlap values. As shown in Sec. 3, many solution communities can be identified in a heterogeneous solution space [17]. Each solution community contains a set of solutions which are more similar with each other than with the solutions of other communities. These differences of intra- and inter-community overlap values and the relative sparseness of solutions at the boundaries between solution communities cause the non-concavity of $s(q)$.

For the random K -SAT problem, we use the replica-symmetric cavity method of statistical mechanics [11] to calculate the mean overlap values $\bar{q}(x)$ at each value of $\alpha < \alpha_d(K)$. As the partition function Eq. (3) is a summation over pairs of solutions $(\vec{\sigma}^1, \vec{\sigma}^2)$, the state of each vertex is a pair of spins (σ, σ') . Details of this calculation can be found in Ref. [16] and here we cite the main results.

Figure 2A shows, for the random 3-SAT problem, the form of the function $\bar{q}(x)$ at several different α values. When $\alpha < \alpha_{cm}(3) \approx 3.75$, the mean overlap \bar{q} increases with the binding field x smoothly, indicating that the entropy density function $s(q)$ is concave in shape (Fig. 1, left panel). The solution space \mathcal{S} of the random 3-SAT problem is then regarded as homogeneous.

When $\alpha > \alpha_{cm}(3)$, there is a hysteresis loop in the $\bar{q}(x)$ curve as the binding field x increases and then decreases around certain threshold value x^* . This behavior is typical of a first-order phase-transition. At $x > x^*$ the partition function $Z(x)$ is contributed mainly by intra-community solution pairs, while at $x < x^*$ it is contributed mainly by inter-community solution pairs.

To determine precisely the critical value α_{cm} , we investigate the overlap susceptibility $\chi \equiv d\bar{q}(x)/dx$, which is a measure of the overlap fluctuations,

$$\chi(x) = \frac{1}{N} \sum_{i=1}^N \sum_{j=1}^N \left[\langle \sigma_i^1 \sigma_i^2 \sigma_j^1 \sigma_j^2 \rangle - \langle \sigma_i^1 \sigma_i^2 \rangle \langle \sigma_j^1 \sigma_j^2 \rangle \right], \quad (5)$$

where $\langle \dots \rangle$ means averaging over solution-pairs under the binding field x . From the divergence of the peak value of $\chi(x)$ as shown in Fig. 2B, we obtain that $\alpha_{cm}(3) = 3.7497$ for the random 3-SAT problem. This value is much below the value of $\alpha_d(3) = 3.87$ [5].

For the random 4-SAT problem, we find that $\alpha_{cm}(4) = 8.4746$. This value is again much below the clustering transition point $\alpha_d(4) = 9.38$ [5]. The difference $\alpha_d(K) - \alpha_{cm}(K)$ appears to be an increasing function of K .

3. Solution graph random walking

For single random K -SAT formulas, the solution space structural heterogeneity can also be detected by performing a long-time random walking in the corresponding solution graphs [22, 23, 19, 17]. The Hamming distance $d(\vec{\sigma}^1, \vec{\sigma}^2)$ between two solutions $\vec{\sigma}^1$ and $\vec{\sigma}^2$ of the solution space is defined as

$$d(\vec{\sigma}^1, \vec{\sigma}^2) = \sum_{i=1}^N \left[1 - \delta(\sigma_i^1, \sigma_i^2) \right] \quad (6)$$

where $\delta(\sigma, \sigma') = 1$ if $\sigma = \sigma'$ and $\delta(\sigma, \sigma') = 0$ if $\sigma = -\sigma'$. This distance counts the number of different spins between the two solutions. The Hamming distance $d(\vec{\sigma}^1, \vec{\sigma}^2)$ is related to the overlap $q(\vec{\sigma}^1, \vec{\sigma}^2)$ [Eq. (2)] through

$$q(\vec{\sigma}^1, \vec{\sigma}^2) = 1 - \frac{2d(\vec{\sigma}^1, \vec{\sigma}^2)}{N}. \quad (7)$$

In the solution graph of a satisfiable random K -SAT formula, a solution $\vec{\sigma}$ is linked to $k_{\vec{\sigma}}$ other solutions, all of which have unit Hamming distance with $\vec{\sigma}$. It was empirically found that the degrees $k_{\vec{\sigma}}$ of the solutions are narrowly distributed with a mean much less than N [17]. The solutions can therefore be regarded as equally important in terms of connectivity. However, the connection pattern of the solution graph can be highly heterogeneous. Even when the whole graph is connected, solutions may still form different communities such that the edge density of a community is much larger than that of the whole graph. The communities may even further organize into super-communities.

Consider two solutions $\vec{\sigma}^1$ and $\vec{\sigma}^2$ of the solution graph. The shortest-path length $l(\vec{\sigma}^1, \vec{\sigma}^2)$ between these two solutions in the solution graph satisfies the inequality $l(\vec{\sigma}^1, \vec{\sigma}^2) \geq d(\vec{\sigma}^1, \vec{\sigma}^2)$. If $\vec{\sigma}^1$ and $\vec{\sigma}^2$ belong to the same solution community, $l(\vec{\sigma}^1, \vec{\sigma}^2)$ may be equal to or just slightly greater than the Hamming distance $d(\vec{\sigma}^1, \vec{\sigma}^2)$. On the other hand, if $\vec{\sigma}^1$ and $\vec{\sigma}^2$ belong to two different solution communities, an extensive spin rearrangement may have to be made to change from $\vec{\sigma}^1$ to $\vec{\sigma}^2$ by single-spin flips, and then $l(\vec{\sigma}^1, \vec{\sigma}^2)$ is much greater than $d(\vec{\sigma}^1, \vec{\sigma}^2)$. If solutions are sampled by a random walking process at equal time interval Δt , the sampled solutions should contain useful information about the community structure of the solution space, with a resolution level depending on Δt . This is because that, when the edges are followed randomly by a random walker, the walker will be trapped in different communities most of the time, and the sampled solutions will then form different similarity groups.

Starting from an initial solution $\vec{\sigma}^0$, a sequences of solutions $(\vec{\sigma}^0, \vec{\sigma}^1, \dots, \vec{\sigma}^l, \vec{\sigma}^{l+1}, \dots)$ are generated by solution graph random walking. Two different random walking processes are used in the simulation. In the *unbiased* random walking process, the solution $\vec{\sigma}^{l+1}$ is a nearest neighbor of solution $\vec{\sigma}^l$ for $l = 0, 1, \dots$ [17]. Under this simple dynamics, if the generated solution sequence is infinitely long, each solution $\vec{\sigma}$ in a connected component of the solution graph will appear in the sequence with frequency proportional to its connectivity $k_{\vec{\sigma}}$. On the other hand, in the *uniform* random walking process, with probability $k_{\vec{\sigma}^l}/N$, the solution $\vec{\sigma}^{l+1}$ ($l = 0, 1, \dots$) is a nearest neighbor of solution $\vec{\sigma}^l$, and with the remaining probability $1 - k_{\vec{\sigma}^l}/N$, solution $\vec{\sigma}^{l+1}$ is identical to $\vec{\sigma}^l$. Under this later dynamical rule, each solution in a connected component of the solution graph will have the same frequency to appear in the generated solution sequence. Both these two random walking processes were used to sample solutions, and the clustering analysis performed on these two sets of data gave qualitatively the same results [17]. The simulation results shown in Fig. 3 were obtained by the unbiased random walking process.

A set of solutions are sampled (with equal time interval Δt) from the generated long sequence of solutions for clustering analysis. (To avoid strong dependence on the input solution $\vec{\sigma}^0$, the initial part of the solution sequence was not used for sampling.) By calculating the overlap values between the sampled solutions, we obtain an overlap histogram as shown in Fig. 3. A hierarchical minimum-variance clustering analysis [24] (see also Ref. [25]) is performed on the sampled solutions. Initially each solution is regarded as a group, and the distance between two groups is the Hamming distance. At each step of the clustering, two groups C_a and C_b that have the smallest distance are merged into a single group C_c . The distance between the merged group C_c and another group C_d is calculated by

$$d(C_c, C_d) = \frac{(|C_a| + |C_d|)d(C_a, C_d) + (|C_b| + |C_d|)d(C_b, C_d) - |C_d|d(C_a, C_b)}{|C_c| + |C_d|}, \quad (8)$$

where $|C|$ is the number of solutions in group C . After the sampled solutions are listed in the order as reported by the minimal-variance clustering algorithm, the matrix of Hamming distances between these solutions are represented in a graphical form as shown in Fig. 3 (upper row).

For a random 4-SAT formula with $N = 20,000$ variables, the overlap histogram and the Hamming distance matrix of 1000 sampled solutions are shown in Fig. 3 for two different constraint density values $\alpha = 9.10$ and $\alpha = 9.22$ in the ergodic phase. At $\alpha = 9.10$, the Hamming distance matrix has a weak signature of the existence of many solution communities, and the overlap histogram is slightly non-concave. At $\alpha = 9.22$, the Hamming distance matrix has a very clear block structure and the overlap histogram is non-monotonic. These observations suggest that the explored solution spaces are heterogeneous both at $\alpha = 9.10$ and $\alpha = 9.22$; the entropic trapping effect of the solution communities becomes much stronger as α increases from 9.10 to 9.22. The simulation results are consistent with the analytical results of the preceding section, they are also in agreement with the expectation that, as $\alpha_d(4)$ is approached from below, a random walker becomes more and more trapped in a single solution community and finally becomes impossible to escape from this single community at $\alpha \geq \alpha_d(4)$.

We have obtained similar simulation results on single random 3-SAT formulas [17]. The solution space random walking simulations confirm that the solution space of the random K -SAT problem is already very heterogeneous before the clustering transition point $\alpha_d(K)$ is reached. The simulation results reported in Ref. [17] also suggested that, at $\alpha > \alpha_d(K)$, the single solution clusters of the solution space of the random K -SAT problem are themselves quite heterogeneous in internal structure, which may be the reason underlying the non-convergence of the belief-propagation iteration process within a single solution cluster [19].

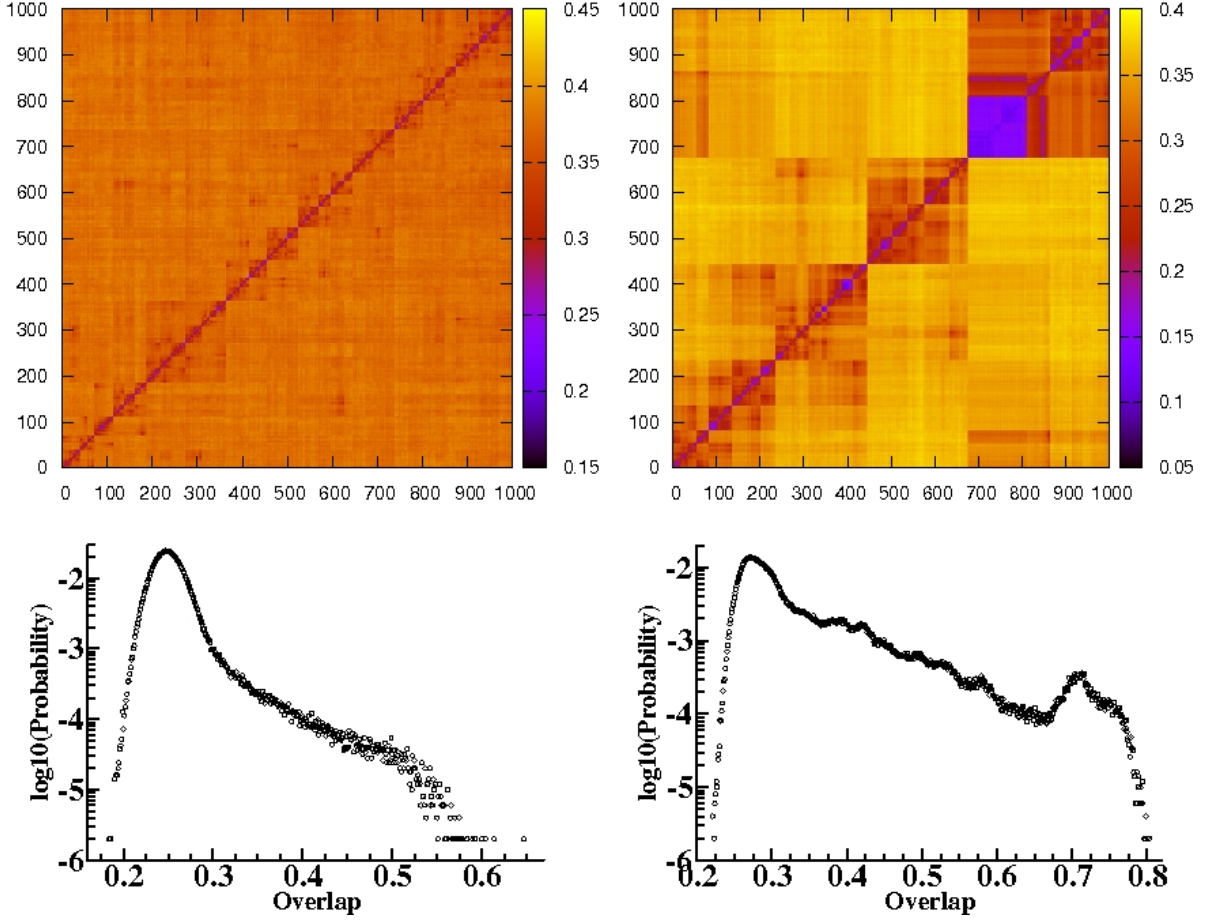


Figure 3. The matrix of Hamming distances of 1000 sampled solutions for a random 4-SAT formula of $N = 20,000$ variables, and the corresponding overlap distribution of these sampled solutions. The solutions were obtained by an unbiased random walking process (solution sampling began after running the random walking process for $3 \times 10^7 \times N$ steps starting from an initial solution, and two consecutively sampled solutions are separated by $\Delta t = 50,000 \times N$ random walking steps). The left panel corresponds to $\alpha = 9.10$ and the right panel to $\alpha = 9.22$. In the Hamming distance matrices, the solutions are ordered according to the results of the minimal-variance clustering analysis.

4. Glassy behavior of a stochastic search algorithm

After a slight change, the solution graph random walking process of the preceding section was turned into a stochastic local search algorithm [18]. This algorithm, referred to as SEQSAT, satisfies sequentially the constraints of a random K -SAT formula F . We denote by F_m the sub-formula containing the first m constraints of F . Suppose a configuration $\vec{\sigma}(t_m)$ that satisfies F_m is reached at time t_m . The $(m+1)$ -th constraint of formula F is added to F_m to obtain the enlarged sub-formula F_{m+1} . Then, starting from $\vec{\sigma}(t_m)$, an unbiased random walk process is running on the solution graph of F_m until a spin configuration $\vec{\sigma}(t_{m+1})$ that satisfies F_{m+1} is first reached at time $t_{m+1} = t_m + \Delta t_m$ after $\Delta t_m \times N$ single-spin flips, N being the total number of variables in formula F . The waiting time of satisfying the $(m+1)$ -th constraint is Δt_m (this time is zero if $\vec{\sigma}(t_m)$ already satisfies F_{m+1}). Starting from a completely random initial spin configuration $\vec{\sigma}(0)$ and an empty sub-formula F_0 , every constraint of the formula F are satisfied

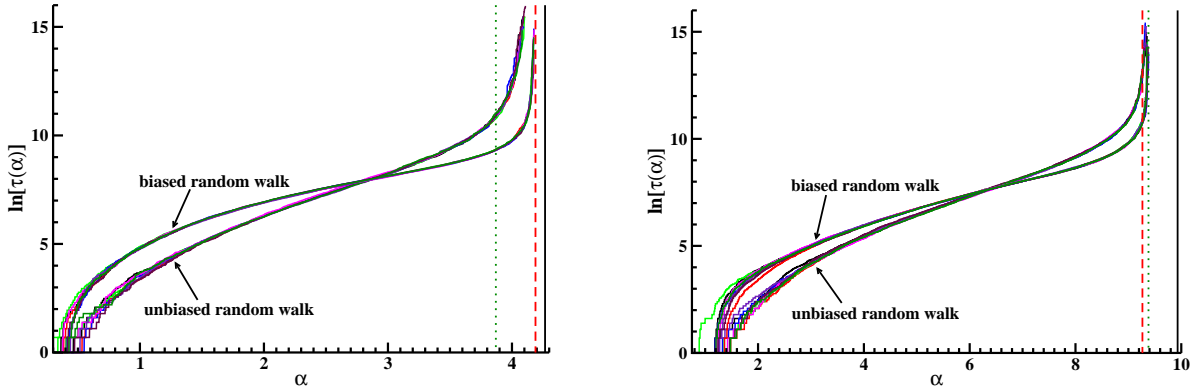


Figure 4. The total search time $\tau(\alpha)$ needed to satisfy the first $\alpha \times N$ constraints of a random K -SAT formula with $N = 100,000$ variables ($K = 3$, left panel; $K = 4$, right panel). The performances of an unbiased random-walk search process and a biased random-walk search process are compared. The red dashed lines correspond to the jamming transition points $\alpha_j(K)$ as predicted by a long-range-frustration mean-field theory [26, 18], the green dotted lines correspond to the clustering transition points $\alpha_d(K)$ [5], and the black solid lines correspond to the satisfiability threshold value $\alpha_s(K)$ [8].

by SEQSAT in this way. Notice that if a constraint was satisfied by SEQSAT, it remains to be satisfied as new constraints are added (energy barrier crossing is not allowed).

Figure 4 shows the simulation results of SEQSAT on a random 3-SAT formula and a random 4-SAT formula, $N = 10^5$. When the constraint density α of the satisfied sub-formula F_m is low, the waiting time needed to satisfy a constraint is very close to zero. As the heterogeneity transition point $\alpha_{cm}(K)$ is reached, however, the waiting time increases quickly and it starts to take more than $100 \times N$ single-spin flips to satisfy a constraint. The search process becomes more and more slow as α further increases. As α approaches another threshold value $\alpha_j(K)$ the waiting time is so long (exceeding $10^6 \times N$ single-spin flips) that SEQSAT essentially stops to satisfy a newly added constraint. The parameter $\alpha_j(K)$ is regarded as the jamming point of the random walk search algorithm. In the range of $\alpha_{cm}(K) < \alpha < \alpha_j(K)$ the SEQSAT is performing an increasingly viscous diffusion in the solution space of the random K -SAT formula. The simulation results of Fig. 4 and those reported in Ref. [18] for single random 5-SAT and 6-SAT formulas clearly demonstrate that, the solution space heterogeneity transition at $\alpha_{cm}(K)$ has significant dynamical consequences for stochastic local search processes.

For the random 3-SAT problem, the jamming point $\alpha_j(3)$ is significantly larger than the clustering transition point $\alpha_d(3)$. At $\alpha_d(3)$ the solution space of a large random 3-SAT formula is dominated by a sub-exponential number of solution clusters [5]. A dominating solution cluster also has internal community structures [17]. As α further increases, a dominating cluster shrinks in size, and it break into many sub-clusters. Figure 4 (left panel) indicates that, the random walker of SEQSAT is residing on one of the dominating clusters at $\alpha \approx \alpha_d(3)$ and it continue to be residing on one of the dominating sub-clusters of the visited cluster as α increases. If the spin values of a large fraction of variables become frozen in the residing solution cluster, a jamming transition then occurs. The value of $\alpha_j(3)$ is predicted to be 4.1897 by a long-range frustration mean-field theory [26, 18], in agreement with the simulation results.

For the random K -SAT problem with $K \geq 4$, the simulation results shown in Fig. 4 (right panel) and in Ref. [18] suggest that the jamming transition point $\alpha_j(K)$ is identical to or very close to the clustering transition point $\alpha_d(K)$. We notice that for the random K -SAT problem

with $K \geq 4$, at $\alpha = \alpha_d(K)$, the union of an exponential number of small solution clusters is contributing predominantly to the solution space [5]. It is expected that, as α approaches $\alpha_d(K)$ from below, the ergodic solution space of a large K -SAT formula is dominated by an exponential number of small solution communities. The solutions reached by SEQSAT probably are residing on one of these small communities. As $\alpha \rightarrow \alpha_d(K)$, each of these small (but statistically relevant) solution communities probably contains a large fraction of variables that are almost frozen.

Figure 4 also shows the performances of a biased random walk search algorithm. The biased random walk process differs from the unbiased random walk process in that, in each single-spin flip, a variable that is flippable but not yet being flipped is flipped with priority [18]. This biased random walk SEQSAT algorithm was implemented with the hope of escaping from a solution community more quickly. For the random 3-SAT and 4-SAT problem, the biased SEQSAT algorithm indeed is more efficient than the unbiased algorithm. But for the random K -SAT problem with $K \geq 5$, the biased algorithm diverges earlier than the unbiased algorithm [18].

5. Conclusion and discussions

The solution space structure of the random K -SAT problem evolves with the constraint density α . Several qualitative transitions occurs in the solution space as α becomes relatively large. We demonstrated, both theoretically and by computer simulations, that the first qualitative structural transition is the heterogeneity transition at $\alpha = \alpha_{cm}(K)$, where exponentially many solution communities start to form in the (still ergodic) solution space. The dynamic behavior of a stochastic search algorithm was investigated. This simple algorithm SEQSAT constructs satisfying spin configurations for a single K -SAT formula by performing a random walk of single-spin flips. Due to the entropic trapping effect of solution communities, the solution space random walking process starts to be very viscous as α goes beyond $\alpha_{cm}(K)$. SEQSAT is able to find solutions for a random K -SAT formula with constraint density less than a threshold value $\alpha_j(K)$. For $K = 3$, the jamming point $\alpha_j(3) \approx 4.19$ is larger than the solution space clustering transition point $\alpha_d(3)$. But for $K \geq 4$, it appears that $\alpha_j(K)$ is very close to $\alpha_d(K)$.

When the constraint density α of a large random K -SAT formula is in the region of $\alpha_{cm}(K) < \alpha < \alpha_d(K)$, the solution space of the formula is heterogeneous but ergodic. If a random walking process is running on the solution space starting from an initial solution, a two-step relaxation behavior can be observed [17], corresponding to a quick slipping into a solution community, a relatively long wandering within this community, and finally the viscous diffusing in the whole solution space. Similar two-step relaxation behaviors were observed in glassy dynamics studies of supercooled liquids (see, e.g., the review article [27]) both in the non-activated dynamics region and in the activated dynamics region.

The existence of solution communities in the solution space may lead to a phenomenon that is similar to the dynamical heterogeneity of supercooled liquids (see, e.g., review articles [28, 29]). For a random walking process on a heterogeneous solution space, if the observation time is less than the typical relaxation time of escaping from the solution communities, one may find that the spin values of a large fraction of variables change only very infrequently among the visited solutions, while the spin values of the remaining variables are flipped much more frequently. The variables of the K -SAT formula then divides into an active group and an inactive group in this observation time window. One may further observe that the active variables are clustered into many distantly separated sub-groups, each of which containing variables that are very close to each other [30]. Numerical simulations need to be performed to investigate in more detail the solution space random walking processes.

The constraint density α of the random K -SAT problem corresponds to the particle density ρ in supercooled liquid. In supercooled liquids, another important control parameter is the temperature T . We can also introduce a positive temperature T to the random K -SAT problem

and investigate how the configuration space evolves with T . It is anticipated that, as T is lowered to a threshold value $T_{cm}(K, \alpha)$ the configuration space will also experience a heterogeneity transition [16]. Detailed theoretical and simulation results will be reported in a later work. For the fully-connected p -spin spherical model of glasses, it has already been shown [32, 33] that a quantity called the Franz-Parisi potential has a change in its concavity property as T is lowered (see [34] for more recent extended studies). Another related problem, the weight space property of the Ising perceptron, was studied in [35]. For this fully connected model, a change of concavity property was also predicted for its characteristic function.

The solution space heterogeneity transition also exists in the random K -XORSAT problem [18]. It may be a general feature of the configuration spaces of spin glass models on finite-connectivity random graphs.

Acknowledgments

The author thanks Kang Li, Hui Ma and Ying Zeng for collaborations. This work was partially supported by the National Science Foundation of China (Grant numbers 10774150 and 10834014) and the China 973-Program (Grant number 2007CB935903).

References

- [1] Kirkpatrick S and Selman B 1994 *Science* **264** 1297–1301
- [2] Achlioptas D 2001 *Theor. Comput. Sci.* **265** 159–185
- [3] Monasson R and Zecchina R 1996 *Phys. Rev. Lett.* **76** 3881–3885
- [4] Mézard M, Parisi G and Zecchina R 2002 *Science* **297** 812–815
- [5] Krzakala F, Montanari A, Ricci-Tersenghi F, Semerjian G and Zdeborova L 2007 *Proc. Natl. Acad. Sci. USA* **104** 10318–10323
- [6] Hartmann A K and Weigt W 2005 *Phase Transitions in Combinatorial Optimization Problems* (Weinheim, Germany: Wiley-VCH)
- [7] Mezard M and Montanari A 2009 *Information, Physics, and Computation* (New York, USA: Oxford Univ. Press)
- [8] Mertens S, Mézard M and Zecchina R 2006 *Rand. Struct. Algorithms* **28** 340–373
- [9] Montanari A, Ricci-Tersenghi F and Semerjian G 2008 *J. Stat. Mech.: Theor. Exp.* P04004
- [10] Zhou H 2008 *Phys. Rev. E* **77** 066102
- [11] Mézard M and Parisi G 2001 *Eur. Phys. J. B* **20** 217–233
- [12] Mézard M and Montanari A 2006 *J. Stat. Phys.* **124** 1317–1350
- [13] Semerjian G 2008 *J. Stat. Phys.* **130** 251–293
- [14] Ardelius J and Zdeborova L 2008 *Phys. Rev. E* **78** 040101(R)
- [15] Gardner E 1985 *Nucl. Phys. B* **257** [FS14] 747–765
- [16] Zhou H 2009 Criticality and heterogeneity in the solution space of random constraint satisfaction problems arXiv:0911.4328 (Int. J. Mod. Phys. B, accepted)
- [17] Zhou H and Ma H 2009 *Phys. Rev. E* **80** 066108
- [18] Zhou H 2010 *Eur. Phys. J. B* **73** 617–624
- [19] Li K, Ma H and Zhou H 2009 *Phys. Rev. E* **79** 031102
- [20] Wasserman S and Faust K 1994 *Social Network Analysis: Methods and Applications* (New York: Cambridge University Press)
- [21] Girvan M and Newman M E J 2002 *Proc. Natl. Acad. Sci. USA* **99** 7821–7826
- [22] Zhou H 2003 *Phys. Rev. E* **67** 041908
- [23] Zhou H 2003 *Phys. Rev. E* **67** 061901
- [24] Jain A K and Dubes R C 1988 *Algorithms for Clustering Data* (Englewood Cliffs, NJ, USA: Prentice-Hall)
- [25] Barthel W and Hartmann A K 2004 *Phys. Rev. E* **70** 066120
- [26] Zhou H 2005 *New J. Phys.* **7** 123
- [27] Cavagna A 2009 *Phys. Report* **476** 51–124
- [28] Ediger M D 2000 *Annu. Rev. Phys. Chem.* **51** 99–128
- [29] Glotzer S C 2000 *J. Non-Cryst. Solids* **274** 342–355
- [30] A random K -SAT formula can be represented by a bipartite graph (see, e.g., Ref. [31]). In this bipartite graph, a circular node represents a variable and a square node represents a constraint, an edge between a variable node i and a constraint node a means that variable i is involved in constraint a . In this bipartite graph, the distance $d(i, j)$ between two variable nodes i and j is defined as the number of constraint nodes

on a shortest-length path between i and j . For example, if i and j both are constrained by the same constraint, then $d(i, j) = 1$; if i and j are not constrained by the same constraint but i and a variable k are involved in constraint a and j and k are involved in constraint b , then $d(i, j) = 2$.

- [31] Kschischang F R, Frey B J and Loeliger H A 2001 *IEEE Trans. Infor. Theor.* **47** 498–519
- [32] Franz S and Parisi G 1995 *J. de Physique I* **5** 1401–1415
- [33] Franz S and Parisi G 1997 *Phys. Rev. Lett.* **79** 2486–2489
- [34] Zdeborova L and Krzakala F 2010 *Phys. Rev. B* **81** 224202
- [35] Obuchi T and Kabashima Y 2009 *J. Stat. Mech.: Theor. Exp.* P12014